

FRACTURE TOUGHNESS DEMANDS IN STANDARD AND REDUCED BEAM SECTION WELDED MOMENT CONNECTIONS

Wei-Ming CHI¹ And Gregory G DEIERLEIN²

SUMMARY

Motivated by widespread cracking in steel structures during the 1994 Northridge earthquake, a detailed finite element investigation is used to examine fracture toughness requirements in welded beam-column connections. Toughness demands are calculated in terms of the elastic stress intensity factor, K_I , and inelastic Crack Tip Opening Displacement, CTOD. The analyses quantify the effects of high localized stresses and strains in the vicinity of weld root defects in beam flange welds of standard connections (representative of pre-Northridge construction) and improved reduced beam section connections. The analyses confirm observations from full-scale connection tests that pre-Northridge connections with large weld root flaws and low toughness E70T-4 weld metal will fracture without significant yielding. Further, the analyses demonstrate that while use of higher toughness materials will improve behavior, this alone does not provide sufficient fracture resistance to ensure levels of ductility required for seismic design. Parametric studies of various connection design parameters (e.g. connection geometry, flaw location, joint panel zone strength/flexibility, use of continuity plates, reduced beam section details) examine how appropriate combinations of these will control fracture toughness demands within tolerable levels for notch-toughness rated welds and base metals.

INTRODUCTION

Following the Northridge and Kobe earthquakes, instances of weld fractures in beam-column connections have been widely reported. Investigations conducted through the SAC Joint Venture (Mahin et al. 1998) and other initiatives have established that premature cracking in welded steel connections resulted from a combination of factors – most notably, high stress and strain demands coupled with large inherent flaws and stress risers, deficient field welding, and over-reliance on low-toughness materials. These created conditions where imposed fracture toughness demands exceeded the available material toughness. Some of these conditions were specific to construction practice in the United States, but the underlying behavioral aspects are universal. Strategies to improve connection behavior include reducing the fracture toughness demand and increasing the available material toughness. Reducing toughness demand can be achieved by minimizing inherent flaws through improved weld details/quality and reconfiguring the connection to reduce stress/strain demands at fracture critical locations. Increasing material toughness can be achieved by using notch-toughness rated welding consumables and stricter adherence to welding procedures that control heat input, cooling rates, and other factors affecting the basic metallurgy of the weld metal and surrounding heat affected zone.

In devising improved connection details and material toughness requirements, one needs an accurate means to determine fracture toughness demands in the connection. Often this is done empirically through large-scale connection tests; however, given the complex interaction of effects and the inherent uncertainties in fracture behavior, connection testing alone is not practical to establish clear cause and effect relationships between various design parameters. Fracture mechanics analyses of the type described herein can play an important role in quantifying toughness requirements and to understand the underlying behavior. The objective of this study is to calculate fracture toughness demands in welded beam-column connections using finite element analyses and, thereby, examine how the connection details influence fracture resistance. Fracture demands are evaluated in terms of stress intensity factor (K_I) and Crack Tip Opening Displacement (CTOD). The study is limited to

¹ Graduate Research Assistant, John A. Blume Earthquake Engineering Center, Stanford University, Stanford, CA 94305-4020

² Associate Professor, John A. Blume Earthquake Engineering Center, Stanford University, Stanford, CA 94305-4020

variations of one basic connection geometry, but it addresses several design parameters including weld flow sizes and location, weld backing bar effects, joint panel zone strength, continuity plates and the effectiveness of reduced beam section (or “dogbone”) details. Moreover, the analyses offer insights that help develop a better intuitive understanding of fracture and how to avoid it.

CONNECTION MODEL AND MATERIALS

The finite element analyses are modeled after the connection detail shown in Fig. 1, which was the subject of a test program conducting during Phase I of the SAC Joint Venture Project (Shuey et al. 1996, Popov et al. 1996). The connection consists of a standard welded-flange bolted-web detail, commonly used in California prior to the Northridge earthquake. As shown in Fig. 2, the typical field welding practice of leaving the weld-backing bar in place creates a built-in flaw behind the backing bar that terminates in the weld. The weld defect size, a_0 , generally varies across the flange width, and is usually largest in the bottom flange beneath the beam-web where welding access is limited and the weld passes terminate.

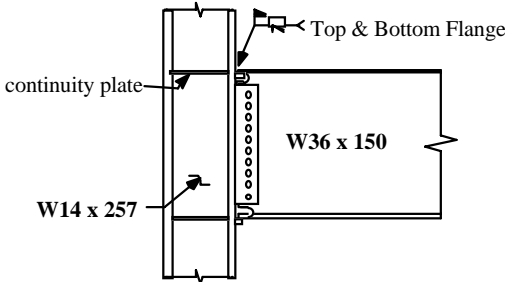


Figure 1 Welded beam-column connection detail

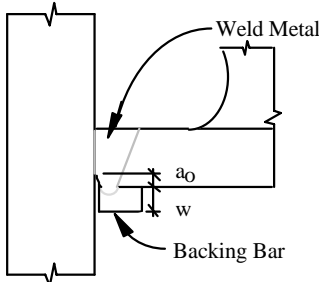


Figure 2 Weld root crack in standard flange weld

Shown in Fig. 3 is one of several finite element models that we used to calculate fracture toughness demands in the connection. This three-dimensional model consists of twenty-node brick elements with eight point integration; other models we have run include two-dimensional models with combinations of plane stress/strain quadrilateral and triangular elements and three dimensional models with mixed shell and solid elements (Chi et.al. 1997, 1999) In all cases, the weld root flaw is modeled as a through-crack running across the full flange width - a simplification of real conditions where the flaw size will vary across the flange width. As shown in Fig. 3, the mesh is highly refined around the crack tip so as to capture the large stress/strain gradients in this region. Of the 15,000 to 25,000 elements in the models, over half are located in close vicinity of the crack tip. Elastic analyses employ singular crack-tip elements and inelastic analyses use collapsed brick elements to model

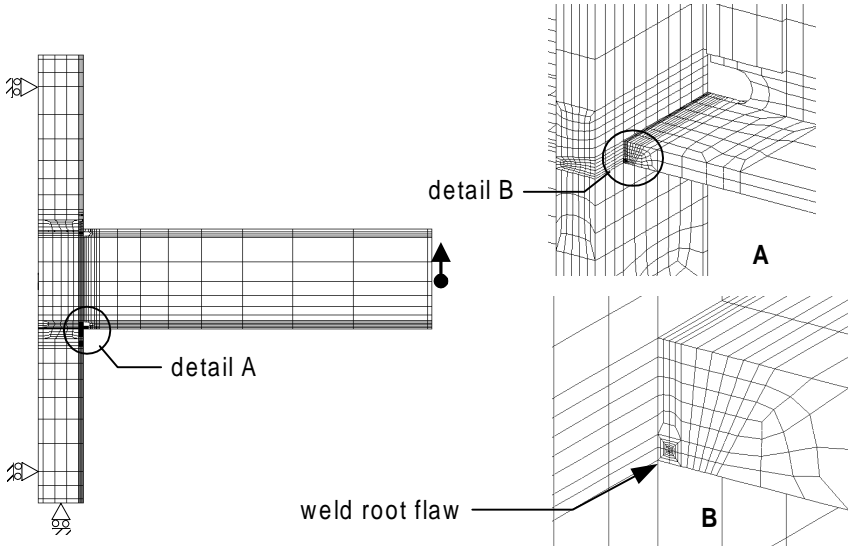


Figure 3 Three-dimensional finite element model with built-in flaw

crack-tip blunting through large strain J-2 plasticity theory with von Mises strain hardening. The analyses were run using the general finite element program ABAQUS (Hibbitt et al. 1997).

Crack tip energy release rates from the analyses were evaluated through a J-integral approach and then converted according to standard fracture theory (Barsom and Rolfe 1987) to mode I stress intensity factor, K_I , for elastic analysis and Crack Tip Opening Displacement, CTOD, for inelastic analyses. These demands can then be compared to critical indices, K_{Ic} and $CTOD_c$, representing fracture toughness of the weld and base metals. Because K_{Ic} and $CTOD_c$ data was not available for materials in the welded beam-column connections, we utilized correlation equations (Barsom and Rolfe 1987) to estimate typical fracture toughness values from the more widely reported Charpy V-Notch (CVN) fracture energy. Shown in Fig. 4, for example, are CVN temperature transition data from tests of two common flux-core welding electrodes (Chi et al. 1999). E70T-4 weld metal that was commonly used prior to the Northridge earthquake has low fracture toughness with lower-shelf CVN energies on the order of 5 to 10 ft-lbs at room temperature (left plot in Fig. 4). On the other hand, electrodes now required for new seismic resistant construction generally provide for more ductile “upper-shelf” behavior. As shown in the right plot of Fig. 4, the notch-toughness rated E70TG-K2 electrode has CVN \approx 70 ft-lb at room temperature. Other notch-tough weld metals in building construction typically have CVN = 40 to 80 ft-lb. For the purpose of interpreting the fracture analyses reported herein, these CVN values for low- and high-toughness materials relate to critical values of K_{Ic} and $CTOD_c$ as follows (Chi et al. 1999):

Lower Toughness: $CVN = 5 \text{ to } 10 \text{ ft-lbs} \Rightarrow K_{Ic} = 40 \text{ to } 60 \text{ ksi}\sqrt{\text{in}} \Rightarrow CTOD_c = 0.0005 \text{ to } 0.0011 \text{ inch}$
Higher Toughness: $CVN = 40 \text{ to } 80 \text{ ft-lbs} \Rightarrow K_{Ic} = 90 \text{ to } 120 \text{ ksi}\sqrt{\text{in}}^{**} \Rightarrow CTOD_c = 0.0024 \text{ to } 0.0042 \text{ inch}^{**}$

Strictly speaking, K_{Ic} and $CTOD_c$ only apply where there is high constraint and small scale yielding around the crack tip. While such conditions are typically met in our analyses at low toughness demands (below $CTOD_c \approx 0.001 \text{ inch}$), at higher toughness demands yielding often encompasses the shallow surface cracks out to the free edge of the material. The resulting loss of crack-tip constraint leads to an increase in the effective toughness of the material beyond the plane strain K_{Ic} and $CTOD_c$ values. Investigations of crack tip constraint, e.g., Sorem et al. 1991, suggest that fracture toughness under low constraint conditions may be on the order of twice that of the high constraint in standard K_{Ic} and $CTOD_c$ tests. Therefore, for assessing the implications of our fracture analyses for higher toughness materials, we would suggest doubling the $CTOD_c$ values indicated above, i.e., for CVN = 40 to 80 ft-lbs the effective toughness would be on the order of $CTOD_c = 0.004 \text{ to } 0.008 \text{ inch}^{**}$ with K_{Ic} correspondingly increasing by $\sqrt{2}$ to $K_{Ic} = 120 \text{ to } 170 \text{ ksi}\sqrt{\text{in}}^{**}$.

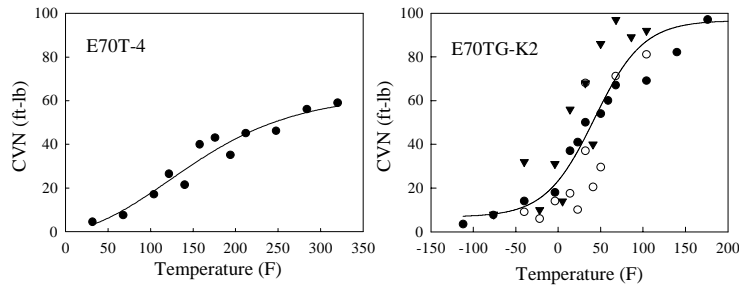


Figure 4 CVN curves for E70T-4 and E70TG-K2 welding electrodes

ELASTIC FRACTURE BEHAVIOR

Shown in Fig. 5 are contour and line plots of longitudinal beam flange stresses in the vicinity of the weld access hole, under an a nominal bending stress of $\sigma_b = M/S = 25 \text{ ksi}$. The line plots are of stresses through the flange thickness calculated by the finite element analysis at the three locations (A,B, and C) and by standard flexural theory, i.e., $\sigma_b = My/I$. The high nonlinearity apparent in the finite element stresses arises due to geometrical discontinuities and localized stress concentrations that are not obvious from conventional “engineering models” of the connection. From the stress distribution at location C, it is apparent that initial flaws located on the lowerface of the beam flange would be more susceptible to fracture than flaws on the inner (upper) face. Thus, referring back to Fig. 2, the largest tensile stress coincides with the tip of the weld root flaw, a_o , above the backing bar gap. Conversely, imagining mirror conditions for the top beam flange, the backing bar gap and weld root on the inside (lower) surface of the beam flange would be subject to very low stresses. These dramatic differences in stresses around the backing bar root flaws help to explain the prevalence of bottom flange versus top flange fractures observed in post-earthquake building inspections and connection tests.

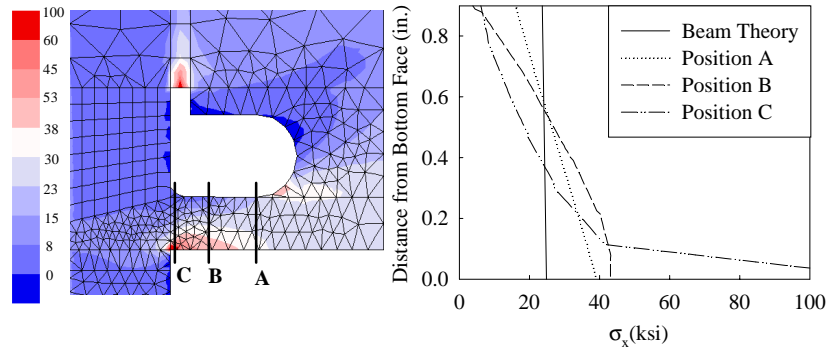


Figure 5 Elastic stress contours in the lower beam flange at the weld access hole

Stress intensity results shown in Figs. 6 to 8 relate the elastic stress state to fracture toughness demands. In these figures, K_I is normalized by the nominal beam bending stress. Data in Figs. 6 and 7 are from two-dimensional analyses while data in Fig. 8 compare two- versus three-dimensional results for a fixed flaw length $a_o = 0.1$ in. In Fig. 6, the stress intensity is related to the weld root flaw length, a_o , for different backing bar thickness, W , where these dimensions are defined in Fig. 2. These plots indicate that K_I is linearly related to flaw length and relatively insensitive to the backing bar thickness W . Data in Fig. 7 show sensitivity of the stress intensity factor to flaw location. Here K_I is fairly constant for various flaws locations across the bottom of the weld (the extreme fiber of the beam) but is about 75% smaller for flaws on the top of the weld (the inside face of the beam flange). This trend follows from the stress distribution shown in Fig. 5 – providing further explanation for the lower incidence of top versus bottom flange fractures. Finally, data in Fig. 8 reveal a significant stress/strain gradient across the beam flange due to shear lag effects. Here K_I at the middle of the flange (beneath the web) is about 1.4 times the average value from two-dimensional analyses. We have run additional analyses that show the ratio $K_{I-3D} / K_{I-2D} = 1.4$ to be fairly constant for a range of member sizes.

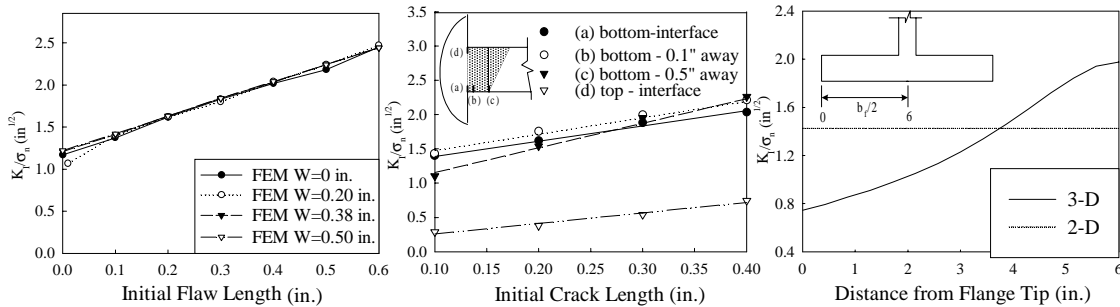


Figure 6 Variation in K_I with flaw and backing bar size

Figure 7 Variation in K_I with locations

Figure 8 2D vs. 3D elastic response

K_I toughness demands from the elastic analysis results in Fig. 6 to 8 can be used to assess whether the beam will reach yield prior to fracture – or alternatively to determine the minimum toughness K_{Ic} required to reach yield. For example, per the 3D results from Fig 8, to reach a nominal beam yield strength of $F_y = 50$ ksi (345 MPa) would require $K_{Ic} > (2.0)(50) = 100$ ksi $\sqrt{\text{in}}$. Accounting for strain hardening and residual stresses, the effective stress demand at the onset of significant plastification would probably increase to about $F_e = 70$ ksi (480 MPa), requiring $K_{Ic} > (2.0)(70) = 140$ ksi $\sqrt{\text{in}}$. Referring back to the metal toughness values indicated previously, demands of $K_{Ic} = 100$ to 140 ksi $\sqrt{\text{in}}$ clearly exceed the fracture toughness of E70T-4 welds and similar low-toughness material but can be resisted by weld and base metals with higher toughness. Predictions of toughness demands beyond the onset of significant yielding requires inelastic analyses that account for both crack tip plasticity and overall yielding behavior of the connection subassembly.

INELASTIC FRACTURE BEHAVIOR

Summarized in this section are inelastic analysis results for the connection detail in Figs. 1 and 2 where the beam and column are assumed to be A572 Grade 50 steel connected with an E70 weld metal. The inelastic models employ average material properties for the base and weld metals reported from other SAC investigations (Chi et al., 1999). According to these studies, expected yield and ultimate strengths for the A572 Gr. 50 base metal are $F_y = 55$ ksi (380 MPa) and $F_u = 73$ ksi (500 MPa). In our analyses, F_u serves as a parameter to characterize the nonlinear isotropic strain hardening model. Strengths for the E70 weld metal are $F_y = 65$ ksi (450 MPa) and

$F_u = 80$ ksi (550 MPa). This combination of base and weld metal results in a slightly overmatched weld ($F_{yw}/F_{yb} = 65/55 = 1.18$), which our previous analyses have shown to be an important factor in reducing fracture demand (crack opening) at the weld root defect above the backing bar (Chi et al. 1997).

Shown in Fig. 9 are fracture toughness demands calculated by a two-dimensional inelastic analysis for the standard connection properties (Fig. 1 and 2) with a weld root defect of $a_o = 0.1$ inch. Plotted on the left is CTOD demand versus applied load (beam moment at the column face), and plotted on the right is CTOD demand versus the plastic connection rotation. For reference, the yield and plastic bending moment capacities of the beam are $M_{yb} = 27,700$ kip-in and $M_{pb} = 32,000$ kip-in, respectively, and the initial yield and ultimate strengths of the column panel zone are $M_{yj} = 26,600$ kip-in and $M_{nj} = 33,300$ kip-in. With the panel zone yield strength less than the plastic moment of the beam, panel zone deformations account for about 70% of the total inelastic connection rotation at $\theta_{inelastic} = 0.03$ radian.

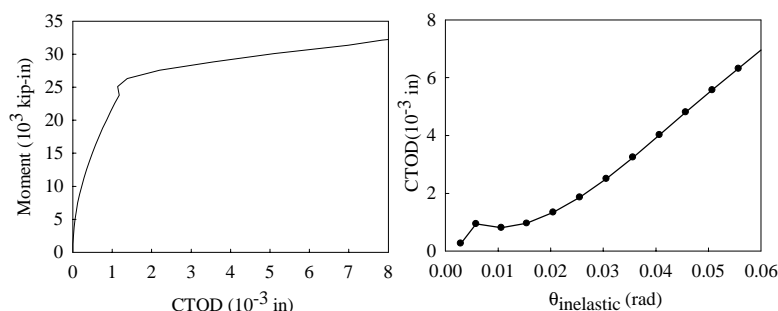


Figure 9 Inelastic fracture demands (2D analysis)

Referring to the left plot in Fig. 9, CTOD begins to rapidly at $CTOD = 0.0015$ with a corresponding moment of $M = 27,000$ kip-in, which is about equal to the yield strength of the joint panel zone. Comparing the left and right plots, when $CTOD = 0.0015$ the plastic rotation is about $\theta_{inelastic} = 0.02$ radian, beyond which CTOD increases almost linearly with plastic connection rotation. Other analyses we have conducted (Chi et al. 1997) indicate that the region of constant CTOD from about $\theta_{inelastic} = 0.005$ to 0.02 radian is due to the beneficial effects of overmatching the weld strength relative to the beam flange strength.

Shown in Fig. 10 are results of additional analyses to explore three-dimensional response and the influence of panel zone deformations and continuity plates on CTOD demand. Plotted in Fig. 10a are data from two-dimensional analyses where the joint panel zone thickness was varied to adjust the ratio of joint panel to beam hinge strength. The three line plots are for CTOD demand at connection deformations of $\theta_{inelastic} = 0.01$, 0.02 and 0.03 radian. The discrete points plotted in Fig. 10a are from three dimensional analyses of two models: the basic case where $M_{nj}/M_{pb} = 1.0$ and another with a strong panel zone where $M_{nj}/M_{pb} = 1.9$. Results from these three-dimensional analyses at $\theta_{inelastic} = 0.03$ are also plotted in Figs. 10b and 10c where, similar to the results in Fig. 8, the variation of CTOD across the beam flange is shown. Figures 10b and 10c also include analysis results for connections without continuity (stiffener) plates. Observations of behavior from these figures follow below.

- Referring to line plots of two-dimensional analyses in Fig. 10a, at the target rotation capacity of $\theta_{inelastic} = 0.03$ radian, the toughness demand sharply decreases with increasing panel zone strength (decreasing panel zone deformations) between $M_{nj}/M_{pb} = 1$ to 2. The peak CTOD demand occurs at $M_{nj}/M_{pb} = 1$ and decreases to about half this amount when $M_{nj}/M_{pb} > 2$, beyond which the panel zone contributes little to the overall connection rotation. Coincidentally, connections with balanced beam and joint panel strengths, i.e., $M_{nj}/M_{pb} = 1.0$, are a common design condition permitted by the AISC Provisions for Seismic Design (1997).
- As with elastic analyses, three-dimensional effects create a non-uniform CTOD demand across the beam flange width, where the maximum value usually occurs in the center beneath the beam web. However, the relative increases are larger for the inelastic analyses. Comparing the discrete points (3D analyses) to the line plots (2D analyses) in Fig. 10a, the peak values from three-dimensional analyses are about 2 to 3 times larger than from two-dimensional analyses.
- Comparing Figs. 10b and 10c, strengthening of the joint panel zone reduces both the peak CTOD demand and the gradient across the beam flange. However, for the case with the strong joint panel (Fig. 10c) there is a spike in CTOD at the flange tip which, in the most extreme cases, exceeds the CTOD beneath the web. This spike may in part be due to the plane stress conditions at the flange tip and “dishing” of the beam

flange. Whether or not the flange tip CTOD represents a critical condition is not certain since (a) the actual flaw size at the flange tip is likely to be smaller than under the beam web, and (b) plane stress conditions at the flange tip will tend to increase the apparent material toughness there.

- Comparing results in Fig. 10b and 10c for connections with and without continuity plates, the column stiffeners decrease the peak CTOD demand by about 0.002 to 0.003 inch. Percentage wise, the reduction is greater in the connection with a strong joint panel (Fig. 10c), but the absolute reduction is greater in the connection with a weak panel zone (Fig. 10b). In this example the column flange thickness is $t_{fc} = 1.9$ inches. Additional parametric analyses we have run on connections with similar beam and column proportions indicate that continuity plates continue to provide a beneficial effect up to column flange thicknesses of about $t_{fc} < 3.5$ inches, beyond which the plates do not seem to make much difference.

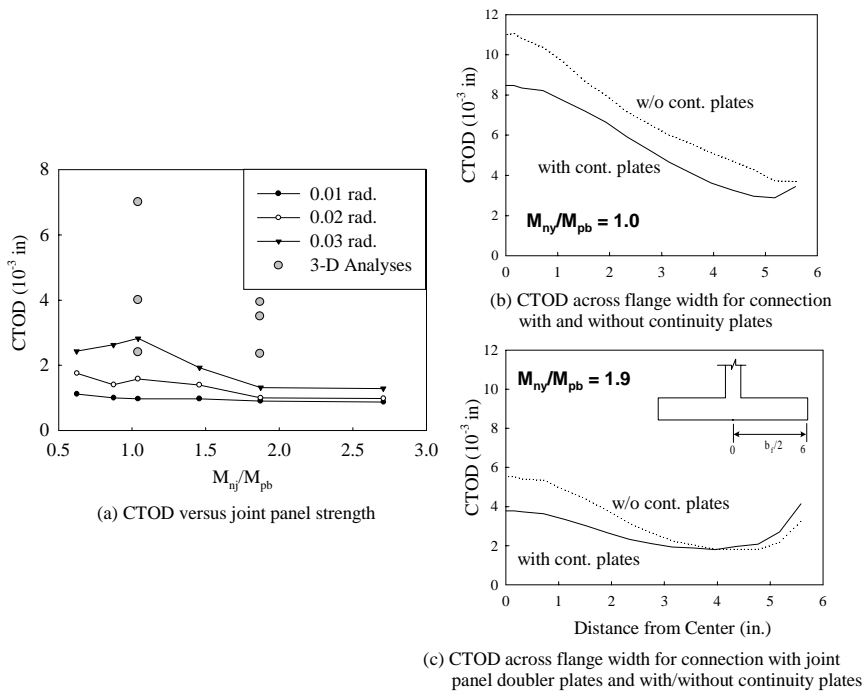


Figure 10 Effects of panel zone strength and continuity plates on CTOD demand

The practical implications of these analyses lie in determining whether or not the connections are likely to fracture prior to reaching the required inelastic rotation for seismic design, currently specified in the AISC Provisions for Seismic Design (1997) as $\theta_{inelastic} > 0.03$ radian for ductile steel moment frames. Referring to Fig. 10b and 10c, the peak CTOD from the three-dimensional analyses range from $CTOD = 0.004$ to 0.011 inch, where the smallest value is for a connection with a strong panel zone and continuity plates. Assuming that high toughness welding electrodes, such as the E70TG-K2, can sustain $CTOD_c = 0.004$ to 0.008 inch for shallow surface cracks, then depending on the specific circumstances, the analysis results suggest that some of the connections would fracture prior to reaching $\theta_{inelastic} = 0.03$ radian. Of course, this assessment is subject to the parameters of the model, including the assumption of an initial weld root flaw of $a_o = 0.1$ inch. Nevertheless, this prediction generally agrees with tests of standard welded connections, where some exceeded the desired inelastic rotation and others did not. Based on such evidence, the general consensus is that, even with high toughness weld metal, conventional details of the type shown in Figs. 1 and 2 do not have adequate fracture resistance for high seismic regions. One way to improve the fracture resistance is through a Reduced Beam Section (RBS) connection detail that is investigated next.

REDUCED BEAM SECTION CONNECTION

Of the many connection alternatives that have been proposed since the Northridge earthquake, one that has emerged as one of the most reliable and practical (economical) is the RBS – or “dogbone” detail (e.g., Englehardt et al. 1998). Similar in many respects to the conventional detail shown in Fig. 1, the main distinguishing feature of the RBS design is a region where the beam flanges are trimmed down a short distance away from the column so as to create a weak fuse region to shield the critical beam flange weld. The effect of this is clearly seen in Fig. 11 where plastic strain contours are compared for the standard connection (Fig. 1) and

an RBS detail where the beam flanges have been trimmed to 50% of their initial width. Whereas the original detail had large panel zone deformations and a concentration of yielding around the beam flange weld, in the RBS design yielding is pushed away from the column.

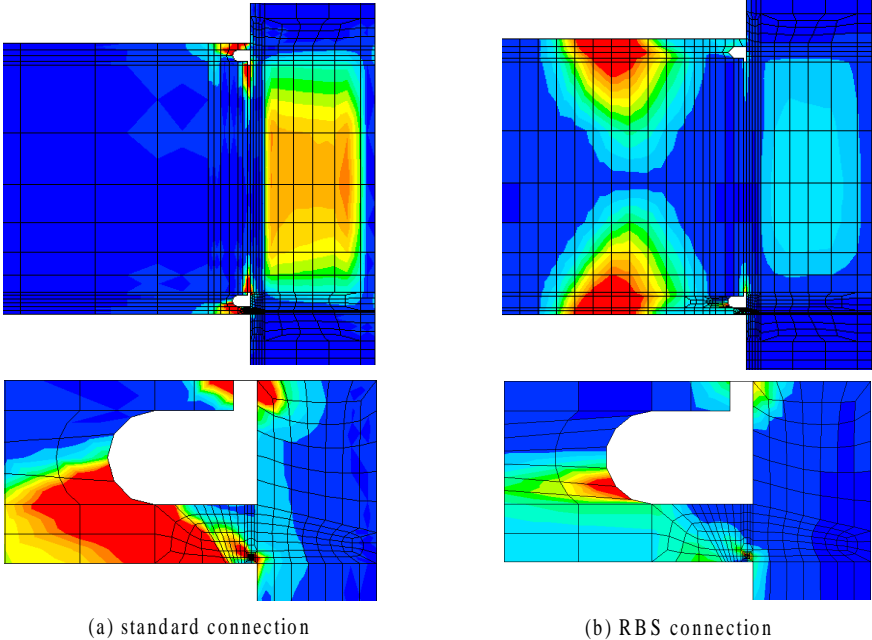


Figure 11 Comparison of effective plastic strain contours of standard and RBS connections

To investigate how effective the RBS detail is in controlling the weld toughness demand, we conducted a number of three-dimensional analyses where the RBS flange reduction was varied between 25% and 50% and the joint panel strength was varied from 1/2 to 2 times its initial value. Recall that the initial joint panel strength is roughly balanced with the beam plastic moment. Results of these analyses, shown in Fig. 12, can be broadly characterized into three groups. The uppermost set of three curves in Fig. 12 includes the standard detail and two RBS designs – one with a 25% RBS reduction and the second with a 50% RBS along with a 0.5 times reduction to the joint panel zone. The similarity of response indicates that the two RBS reductions are not large enough to significantly limit panel zone deformations to the point of reducing CTOD demand below what occurs in the standard connection. Conversely, the set of the three lowest curves indicate that CTOD demand can be constrained to $CTOD < 0.004$ inch when the RBS reduction is large enough. Here the three lowest curves are two 50% RBS details with strong panel zones (1.5 and 2.0) and the 25% RBS with a strong (2x) panel zone. Between the low and high sets of curves are two curves (the standard detail with a strong panel zone and the 50% RBS detail with the original panel zone) with intermediate fracture toughness demands.

One can conclude from the data in Fig. 12 that with proper balance between the RBS reduction relative to the joint panel zone, the CTOD demands can be contained below $CTOD < 0.004$ inch which is within the toughness range that most notch-tough weld metals can provide. On the other hand, without sufficient RBS reduction to minimize panel zone deformations, toughness demands in the RBS detail can be as large as in the standard detail. Keep in mind, of course, that CTOD demands in Fig. 12 are calculated for assumed 0.1 inch root weld defects. The demands can vary for different size flaws and flaws at other locations.

CONCLUDING REMARKS

Seismic design of welded beam-column connections requires a sound understanding of factors that influence their fracture resistance. Quantifying fracture toughness demands is one aspect of the problem; the other is to know the fracture toughness of the material – including the weld and metals and heat affected zones. Limited in scope to fractures initiating from weld-root defects and subject to the many simplifications and assumptions in the finite element fracture models, this study has shown relationships between flaw location, panel zone deformations, continuity plates, and RBS flange reductions on fracture toughness demands. We are currently investigating other parameters as part of the larger SAC Joint Venture effort. There are many uncertainties in the problem that make accurate prediction of fracture difficult, including large variations in material properties, lack of test data on fracture toughness properties, and approximations/limitations in the fracture mechanics analyses

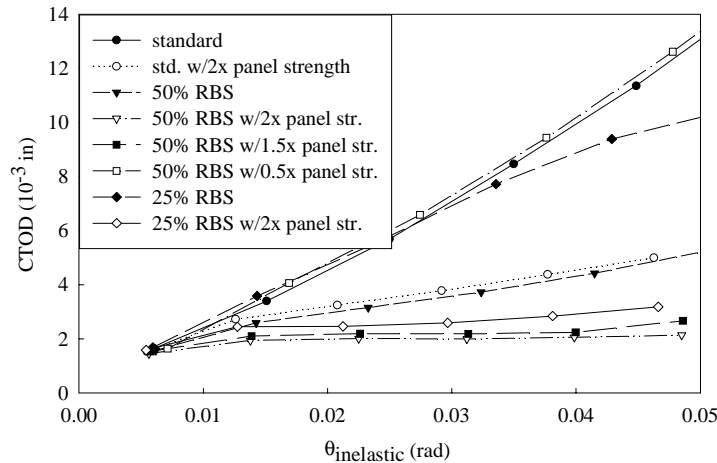


Figure 12 CTOD demands of connections with combinations of RBS details and joint panel strength

Nevertheless, analyses of the type reported here provide an effective means to evaluate the likelihood of fracture and how it is influenced by various design and detailing parameters. We hope that this study will motivate further understanding and development of practical design concepts that incorporate fracture mechanics principles to ensure ductile response of welded steel structures.

ACKNOWLEDGEMENTS

This study was supported by the SAC Joint Venture through a contract from the Federal Emergency Management Agency. The authors gratefully acknowledge valuable suggestions and sharing of data by members of the SAC Management Team and Technical Committees, in particular James Malley, Stephen Mahin, Ron Hamburger, Charles Roeder, Robert Dodds, John Barsom, Mathew Johnson, and Karl Frank. The authors would also acknowledge the contributions of Anthony Ingraffea who participated in an earlier phase of this project. The authors are solely responsible for the results, statements, and interpretations contained in this paper.

REFERENCES

- American Institute of Steel Construction, (1997), "Seismic Provisions for Steel Buildings," AISC, Chicago, IL.
- Barsom, J.M., Rolfe, S.T. (1987), *Fracture and Fatigue Control in Structures - Applications of Fracture Mechanics*, Prentice Hall, Englewood Cliffs, NJ.
- Chi W-M, Deierlein, G.G., Ingraffea, A.R. (1997), *Finite Element Fracture Mechanics Investigation of Welded Beam-Column Connections*, SAC/BD-97/05, NISEE, Berkeley, CA.
- Chi W-M, Deierlein, G.G., (1999), "Integrative Analytical Investigations on the Fracture Behavior of Welded Moment Resisting Connections," SAC Project Report, in preparation (contact ggd@stanford.edu)
- Englehardt, M.D. et al. (1998), "Exper. Invest. of Dogbone Moment Conn.," *Engr. JI.*, AISC, 35(4), pp. 128-139.
- Hibbitt, Karlsson and Sorenson (1997), *ABAQUS/Standard 1, Version 5*, Pawtucket, RI.
- Mahin, S.A., Hamburger, R.O., Malley, J.O. (1998), "National Program to Improve Seismic Performance of Steel Frame Buildings," *Jl. Perf. of Const. Facilities*, ASCE, 12(24), pp. 172-179.
- Popov, E.P., Blondet, M., Stepanov, L., Stojadinovic, B. (1996), "Full Scale Steel Beam-Column Connection Tests," SAC Technical Report 96-01, Part 2, SAC Joint Venture, Sacramento, CA., pp. 4-1 to 4-129.
- Shuey, B.D., Engelhardt, M.D., Sabol, T.A. (1996), "Testing of Repair Concepts for Damaged Steel Moment Connections," *SAC Technical Report 96-01*, Part 2, SAC Joint Venture, Sacramento, CA., pp. 5-1 to 5-332.
- Sorem, W.A., Dodds, R.H., Rolfe, S.T. (1991), "A Comparison of the J-Integral and CTOD Parameters for Short Crack Specimen Testing," *Elastic-Plastic Fracture Test Methods*, ASTM STP 1114, pp. 19-41.